Elastic Constants of AlLi from First Principles

Tokuteru Uesugi*, Yorinobu Takigawa and Kenji Higashi

Department of Metallurgy and Materials Science, Graduate School of Engineering, Osaka Prefecture University, Sakai 599-8531, Japan

The elastic stiffness coefficients of single crystal AlLi with cubic NaTl ($B32$) structure were calculated at 0 K from the first principles. The obtained elastic stiffness coefficients, in units of GPa, were $c_{11} = 66.9$, $c_{12} = 38.2$ and $c_{44} = 51.7$. Then the bulk modulus, Young's modulus, shear modulus and Poison's ratio were estimated for polycrystalline AlLi from the elastic stiffness coefficients. The Young's modulus for single crystal AlLi was the highest in the $\langle 111 \rangle$ direction. The formation of the sp^3-like bond connecting the nearest-neighbor Al atoms was confirmed from the charge density distribution. The elastic anisotropy of AlLi was compared with those of the sp^3 bonded semiconductors such as Si and GaAs.

1. Introduction

AlLi is an intermetallic compound with cubic NaTl ($B32$) structure (space group $Fd\bar{3}m$ No. 227). Its lattice parameter has been determined by several researchers.[1–4] The structure of AlLi is composed of two sublattices, both Al and Li forming a diamond lattice and interpenetrating each other. If Li gives up its single valence electron and the charge is transferred from Li to more electronegative Al, Al has four electrons to form sp^3 bonds.[5,6] A number of studies have been reported on the electronic structure of AlLi because of this peculiar bonding property.[7–10] AlLi is also known as the precipitate of stable δ phase in Al–Li alloys. In Al–Li alloys metastable δ' (Al$_3$Li) phase nucleates during quenching or aging on the grain boundaries or homogenously.[11–13] Metastable δ' phase plays a significant role in the precipitation hardening.[11–13] As aging proceeds, more and more precipitations of new δ' phases with coarsening of existing δ' phase nuclei increase strength.[11–13] After continuing aging, or increase in aging temperature, δ phase nucleates on grain boundaries or already existing δ' phases with dissolution of δ' phases.[11–13] Hence, the first-principles approaches for the study of phase transformation from metastable δ' phase to stable δ phase have been of special interest.[14–18] Large δ phases on grain boundaries cause the marked problem of grain boundary fracture in Al–Li alloys.[19,20] The elastic constants of the precipitate is useful to predict fracture toughness of alloys.[21–23] Hence, it is important to determine elastic constants of AlLi from the viewpoint of material engineering.

The first-principles calculations based on the density functional theory (DFT) have been remarkably successful in the reproducing and explaining a wide variety of materials phenomena.[10,14–18,24–41] The elastic constants have been calculated from the first principles for many alloys and intermetallic compounds.[24–27,35–41] For examples, Masuda-Jindo and Terakura calculated the bulk moduli of Al–Li solid solutions against the solute concentration of Li and Mehl calculated the pressure dependence of the elastic stiffness coefficients of Al$_3$Li.[24,26] In the case of AlLi, its bulk modulus has been calculated by several researchers theoretically,[10,16–18] and the bulk modulus, Young's modulus, shear modulus and Poison's ration were measured on a polycrystalline specimen experimentally.[3] However, the elastic stiffness coefficients of single crystal AlLi have been not investigated both theoretically and experimentally. In the present paper, the elastic stiffness coefficients of single crystal AlLi were determined at 0 K from the first principles. The elastic moduli such as bulk modulus and Young's modulus were estimated for polycrystalline AlLi using the Voigt–Reuss–Hill averaging scheme from the elastic stiffness coefficients.

2. Calculation Methods

The elastic constants determine the stiffness of a crystal against an externally applied strain. For small deformations a linear dependence of the stress on the strain is observed (Hooke's law). Hooke's law can be generalized to account for multiaxial loading conditions as well as the elastic anisotropy. For the cubic structure such as AlLi, the number of independent components of the elastic stiffness tensor is three (c_{11}, c_{12} and c_{44}) and the generalized Hooke's law can be written as

$$\begin{pmatrix} \sigma_{xx} \\ \sigma_{yy} \\ \sigma_{zz} \\ \sigma_{xy} \\ \sigma_{yz} \\ \sigma_{zx} \end{pmatrix} = \begin{pmatrix} c_{11} & c_{12} & c_{12} & 0 & 0 & 0 \\ c_{12} & c_{11} & c_{12} & 0 & 0 & 0 \\ c_{12} & c_{12} & c_{11} & 0 & 0 & 0 \\ 0 & 0 & 0 & c_{44} & 0 & 0 \\ 0 & 0 & 0 & 0 & c_{44} & 0 \\ 0 & 0 & 0 & 0 & 0 & c_{44} \end{pmatrix} \begin{pmatrix} \varepsilon_{xx} \\ \varepsilon_{yy} \\ \varepsilon_{zz} \\ \varepsilon_{xy} \\ \varepsilon_{yz} \\ \varepsilon_{zx} \end{pmatrix}, \quad (1)$$

where σ_{ij} and ε_{ij} ($i, j = x, y, z$) are the stress and strain, respectively. The relationship between the stress and strain is determined by the first-principles calculations. The elastic stiffness coefficients are then obtained from the slope of the stress versus strain. A set of two independent calculations has been performed for AlLi for the following strain conditions:

(1) The first condition: an uniaxial strain ε_{xx} with $\varepsilon_{yy} = \varepsilon_{zz} = \varepsilon_{xy} = \varepsilon_{yz} = \varepsilon_{zx} = 0$. c_{11} is determined from the

---

relationship between σ_{xx} and ε_{xx}. c_{12} is determined from the relationship between $\sigma_{yy} = \sigma_{zz}$ and ε_{xx}.

(2) The second condition: a pure shear strain ε_{xy} with $\varepsilon_{xx} = \varepsilon_{yy} = \varepsilon_{zz} = \varepsilon_{yz} = \varepsilon_{zx} = 0$. c_{44} is determined from the relationship between σ_{xy} and ε_{xy}.

The first-principles calculations presented in this paper were performed using the Cambridge Serial Total-Energy Package (CASTEP).[42] The CASTEP is an *ab initio* pseudo-potential method code for the solution of the electronic ground state of periodic systems with the wave functions expanded in plane wave basis using a technique based on the density functional theory (DFT).[43,44] The electronic ex-change-correlation energy was given by the generalized gradient approximation (GGA) (PW91) of Perdew *et al.* in the DFT.[45] Troullier–Martins pseudopotentials were used for Al,[46] and an ultra-soft pseudopotential was used for Li.[47] The cut-off energy of 350 eV for plane-wave basis was used for all calculation. The energy integration over a Brillouin zone was made with k-point grids according to the Monkhorst–Pack sets of $6 \times 6 \times 6$ k-points for the cubic AlLi unit cell containing 16 atoms.[48]

The stable atomic configurations were obtained through relaxation according to the Hellmann–Feynman forces. Relaxation of the internal degrees of freedom was carried out in the case of all elastic stiffness coefficients. This relaxation is necessary because the atomic positions are not completely fixed by the space group symmetry. The distortion of the crystal causes the reduction of its symmetry. Therefore, there exist free internal parameters that must be redetermined for any distortion of the crystal.

The stress tensor was evaluated using formalism of Nielsen and Martin.[49,50] Nielsen and Martin have derived the reciprocal-space expression of the stress.[49,50] The stress $\sigma_{\alpha\beta}$ is derived from the total energy E_{tot} per a unit-cell volume Ω applying the scaling $r \to (I + d\varepsilon)r$, r are the real lattice vectors. The expression for the stress is

$$\sigma_{\alpha\beta} = \frac{1}{\Omega}\frac{\partial E_{tot}}{\partial \varepsilon_{\alpha\beta}} \qquad (2)$$

where $\varepsilon_{\alpha\beta}$ is the strain tensor. It is to be noted that the strain tensor transforms the reciprocal lattice vectors G to $(I - d\varepsilon)G$ and detailed expressions of the total energy are can be found in the references.[42,49,50]

3. Results and Discussion

At first, the equilibrium lattice constant of AlLi was calculated by use of a Broyden-Fletcher-Goldfarb-Shanno (BFGS) minimization algorithm,[51] and then the elastic stiffness coefficients at the equilibrium lattice constant were calculated. Figure 1 shows the calculated stress for the different strain for each of the two conditions. The values of c_{11}, c_{12} and c_{44} were routinely obtained from the calculated results. The calculated results including the lattice constant with its experimental value are presented in Table 1.[3] The equilibrium lattice constant at 0 K of the cubic AlLi unit cell containing 16 atoms is $a = 0.6295$ nm. The error of the equilibrium lattice constant between the calculated and experimental value is about -1.3%. The relaxation of the internal degrees of freedom has been carried out in the results
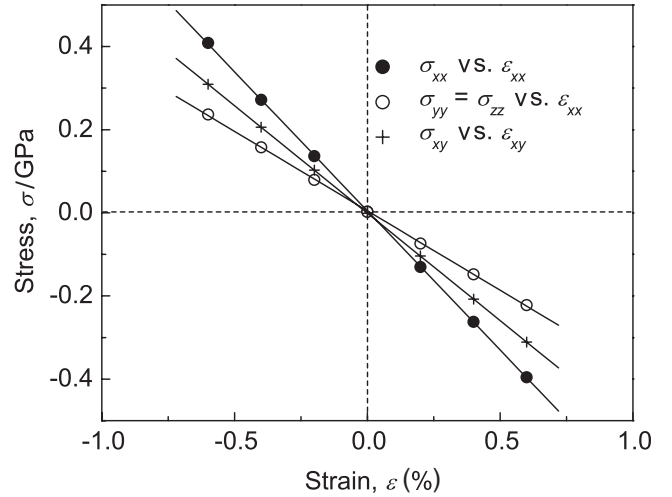

Fig. 1 The relationship between σ_{xx} and ε_{xx} (●) and the relationship between $\sigma_{yy} = \sigma_{zz}$ and ε_{xx} (○) in the first condition (uniaxial strain ε_{xx} with $\varepsilon_{yy} = \varepsilon_{zz} = \varepsilon_{xy} = \varepsilon_{yz} = \varepsilon_{zx} = 0$) and the relationship between σ_{xy} and ε_{xy} (+) in the second condition (pure shear strain ε_{xy} with $\varepsilon_{xx} = \varepsilon_{yy} = \varepsilon_{zz} = \varepsilon_{yz} = \varepsilon_{zx} = 0$).

Table 1 The calculated lattice constant a and elastic stiffness coefficients, c_{11}, c_{12} and c_{44}, of single crystal AlLi from the first principles and the isotropic elastic constants — the bulk modulus B, shear modulus G, Young's modulus E and Poisson's ratio ν — of polycrystalline AlLi calculated from the elastic stiffness coefficients with the Voigt–Reuss–Hill averaging scheme. Available theoretical and experimental values are also listed for the comparison.[3,17]

	This work	FLAPW[17]	Experiment[3]
a (nm)	0.6295	0.6256	0.6377
c_{11} (GPa)	66.9		
c_{12} (GPa)	38.2		
c_{44} (GPa)	51.7		
B (GPa)	47.8	57.75	50.7
G (GPa)	31.0		16.6
E (GPa)	76.6		44.9
ν	0.23		0.35

shown in Table 1. This relaxation can induce significant changes in the magnitudes of the elastic stiffness coefficients. Beckstein *et al.* calculated the elastic stiffness coefficients of single crystal Pt_2Si and PtSi from the first principles.[35] They reported this relaxation induced increases and decreases in the values of the elastic stiffness coefficients up to 20%.[35] In the cases of AlLi, all elastic stiffness coefficients are unchanged within numerical uncertainties, however. To our knowledge, there have been no experimental and theoretical values of the elastic stiffness coefficients on single crystal AlLi. We should therefore consider the elastic moduli such as the bulk modulus and Young's modulus, for the comparison with experimental results.

From the results of the elastic stiffness, the bulk modulus B, Young's modulus E, shear modulus G, Poisson's ratio ν were determined using the Voigt–Reuss–Hill averaging scheme.[36,52–54] In the Voigt average, the shear modulus in the cubic system is given by

$$G_V = \frac{c_{11} - c_{12} + 3c_{44}}{5}, \qquad (3)$$

while in the Reuss average it is given by

$$G_R = \frac{5(c_{11} - c_{12})c_{44}}{4c_{44} + 3(c_{11} - c_{12})}. \qquad (4)$$

The bulk modulus B is the same in both the Voigt and Reuss averages in the cubic system and it is given by

$$B = \frac{c_{11} + 2c_{12}}{3}. \qquad (5)$$

If the Voigt and Reuss averages are applied to calculate average isotropic elastic moduli for polycrystalline using the elastic stiffness coefficients, they give the theoretical maximum (Voigt average) and minimum (Reuss average) values of isotropic elastic moduli.[36,52] Frequently, their arithmetic average $G = (G_V + G_R)/2$ is taken for an estimation of the elastic modulus.[36,52] The other two elastic constants describing an isotropic polycrystalline material, the Young modulus E and Poisson's ratio ν, can be expressed as

$$E = \frac{9GB}{3B + G} \qquad \nu = \frac{3B - 2G}{2(3B + G)}. \qquad (6)$$

The bulk modulus B, Young's modulus E, shear modulus G and Poisson's ratio ν are shown in Table 1. Table 1 includes another theoretical value of the bulk modulus calculated by the first-principles full-potential linearized augmented-plane-wave (FLAPW) method within the local-density approximation (LDA),[17] and experimental values of the bulk modulus, Young's modulus, shear modulus and Poisson's ratio measured by the ultrasonic pulse-transmission technique on a polycrystalline specimen at room temperature.[3] The bulk modulus calculated by the FLAPW method within the LDA is lager by 13.9% than the experimental value while our calculated bulk modulus by *ab initio* pseudopotential method within the GGA is in good agreement with the experimental value: the difference of the bulk modulus between our calculated and experimental value is about −5.7%. It is well known that the elastic moduli calculated from the first principles within the LDA are larger than the experimental values and the GGA calculations have been found to improve the LDA results as shown in this work.

While the calculated bulk modulus is in good agreement with the experimental value, the calculated shear modulus and Young's modulus are lager by 86.7% and 70.6% than experimental values, respectively. The Voigt–Reuss–Hill averaging scheme assumes that the number of grains is sufficiently large and the orientations are randomly distributed. On the other hand, the number of grains and texture affect any elastic moduli except bulk modulus in real polycrystalline materials. So some researchers has developed the methods to calculate the contribution of the number of grains and texture to the anisotropy of the elastic moduli of polycrystalline materials.[55–57] A lot of average isotropic elastic moduli for isotropic polycrystalline materials have been calculated using the Voigt–Reuss–Hill averaging scheme from the elastic stiffness coefficients of the single crystals that were determined not only from the first-principles calculations but also from the experimental mesu-

ments.[27,35–41,52–55,57–59] In many cases, the values of the average isotropic elastic moduli have been in good agreement with the values measured on polycrystalline specimens experimentally.[53–55] However, they were not always in good agreement with the experimental values. In the case of InLi the structure of which is NaTl structure same as AlLi, the average elastic moduli were different from the experimental values.[3,60] Kuriyama *et al.* determined the elastic stiffness coefficients of single crystal InLi by an ultrasonic pulse-transmission technique and reported the average Young's modulus of polycrystalline InLi, which was calculated from their elastic stiffness coefficients, was 38.75 GPa.[60] They also measured the Young's modulus of InLi on a polycrystalline specimen by the same experimental technique after a few years.[3] They reported the Young's modulus measured on a polycrystalline specimen was 67.8 GPa, which was different from the average Young's modulus determined by the same researchers by about 75%.[3,60] InLi and AlLi exhibit large elastic anisotropies as described later. Therefore, the elastic moduli of these polycrystalline materials are sensitive to the number of grains and/or the texture. It seems to be difficult to compare the average elastic moduli calculated using the Voigt–Reuss–Hill averaging scheme with the experimental values measured on polycrystalline specimens in large anisotropy materials such as InLi and AlLi. It is concluded that the experimental values of the elastic stiffness coefficients of single crystal AlLi, which have not been reported, are required in order to compare the elastic constants calculated in this work with the experimental values.

The orientation dependence of the Young's modulus on a single crystal can be obtained from the elastic compliance coefficients s_{ij}. For the case of the cubic system, it can be shown that the Young's modulus in any given direction is given in terms of the three independent elastic compliance coefficients and the direction cosines of the crystallographic direction:

$$\frac{1}{E} = s_{11} - 2\left[(s_{11} - s_{12}) - \frac{1}{2}s_{44}\right](l_1^2 l_2^2 + l_2^2 l_3^2 + l_1^2 l_3^2), \quad (7)$$

where l_1, l_2 and l_3 are direction cosines and s_{11}, s_{12} and s_{44} are obtained by the relation ships $c_{44} = 1/s_{44}$, $c_{11} - c_{12} = (s_{11} - s_{12})^{-1}$ and $c_{11} + 2c_{12} = (s_{11} - 2s_{12})^{-1}$ in the cubic system. Figure 2 shows the orientation dependence of the Young's modulus for single crystal AlLi. The orientation dependence of the Young's modulus was calculated by rotating from the [001] to [00$\bar{1}$] direction around the [100] and [1$\bar{1}$0] axes, respectively. The value of the Young's modulus for the $\langle 111 \rangle$ direction is the highest in all direction and about three times as large as that for the $\langle 100 \rangle$ direction. This means that single crystal AlLi exhibits a large elastic anisotropy. This large elastic anisotropy is considered to be closely related to the interatomic bonding strength.

To illustrate the nature of the bonding it is shown that the three-dimensional representation of the charge density distribution for AlLi in Fig. 3. This figure clearly shows an interesting feature of pronounced Al–Al bonds connecting the nearest-neighbor Al atoms of the Al diamond-type sublattice just like sp^3 bond in Si and GaAs. Earlier researchers also reported the formation of this sp^3-like bond connecting the nearest-neighbor Al atoms from their band
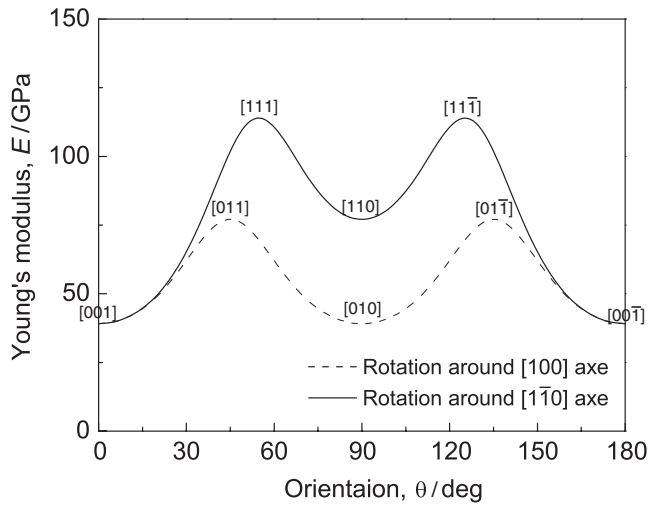
Fig. 2 The orientation dependence of the Young's modulus for single crystal AlLi.

Fig. 3 Three-dimensional representation of the charge density distribution for AlLi. The gray isosurface indicates the surface of isovalue of the charge density 225 nm^{-3}. The black and white balls indicate Al and Li atoms, respectively.

Table 2 The ratio of the Young's modulus for the $\langle 111 \rangle$ direction to that for the $\langle 100 \rangle$ direction, namely E_{111}/E_{100}, of Si, Ge, GaAs, InSb, AlLi and InLi. Si, Ge, GaAs and InSb are semiconductors with diamond or ZnS structure. On the other hands, AlLi and InLi are semimetals with NaTl structure. The Young's moduli of Si, Ge, GaAs, InSb and InLi are calculated from the elastic stiffness coefficients that are experimental values in references.[60-64]

	Si[61]	Ge[64]	GaAs[62]	InSb[63]	AlLi	InLi[60]
E_{111}/E_{100}	1.44	1.51	1.66	1.82	2.91	3.31

calculations.[8,10,16] It is noted that the bond in AlLi is weaker than that in Si and GaAs, while the bonding nature in AlLi is similar to that in Si and GaAs. This is because that the bond length of AlLi is shorter than those of Si and GaAs.[3,16] The sp^3-like bond in AlLi consists with the elastic anisotropy of single crystal AlLi: the direction of the nearest-neighbor Al–Al bonds is $\langle 111 \rangle$ in which the value of the Young's modulus is the highest as shown in Fig. 2.

It is interesting to compare the elastic anisotropy of AlLi with the sp^3 bonded semiconductors such as Si and GaAs. Table 2 shows the ratio of the Young's modulus for the $\langle 111 \rangle$ direction to that for the $\langle 100 \rangle$ direction, namely an elastic anisotropy E_{111}/E_{100}, of Si, Ge, GaAs, InSb, AlLi and InLi. Si, Ge, GaAs and InSb are the sp^3 bonded semiconductors with diamond or ZnS structure. On the other hands, AlLi and InLi are semimetals with NaTl structure.[3] The sp^3-like bonds are expected to form in InLi as in the case of AlLi.[5,6] As can be seen from Table 2, the elastic anisotropy E_{111}/E_{100} of AlLi and InLi is lager than those of the sp^3 bonded semiconductors with diamond or ZnS structure. In the case of AlLi, several researchers reported that the nearest-neighbor Al–Li bond along $\langle 111 \rangle$ direction is the ionically polarized covalent bond and the Li–Li bond is nonbonding from their band calculations.[7,9] This Al–Li bond is expected to contribute to the elastic anisotropy of AlLi in addition to the sp^3-like Al–Al bond.
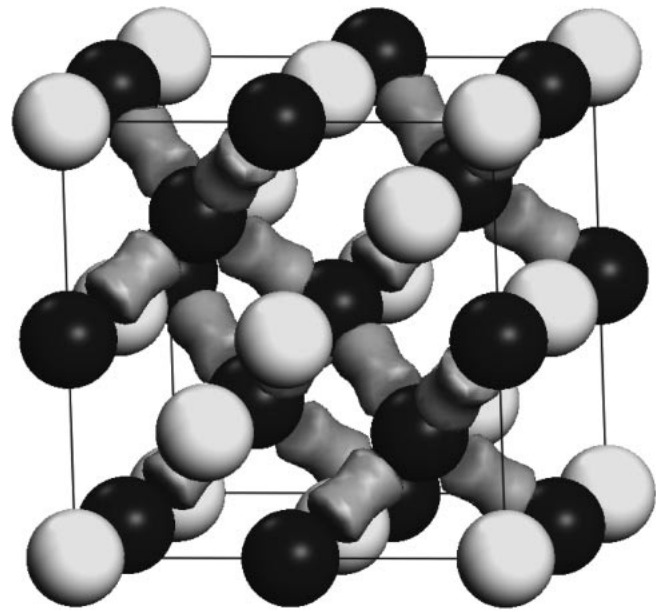
4. Summary

(1) The elastic stiffness coefficients of single crystal AlLi with cubic NaTl ($B32$) structure were calculated at 0 K from the first principles. The obtained elastic stiffness coefficients, in units of GPa, were $c_{11} = 66.9$, $c_{12} = 38.2$ and $c_{44} = 51.7$.

(2) The bulk modulus B, Young's modulus E, shear modulus G and Poison's ratio ν were estimated for polycrystalline AlLi using the Voigt–Reuss–Hill averaging scheme from the elastic stiffness coefficients. The calculated elastic moduli were compared with experimental values measured on a polycrystalline specimen at room temperature. While the calculated bulk modulus was in good agreement with experiment value, the calculated shear modulus and Young's modulus were lager by 86.7% and 70.6% than experimental values, respectively.

(3) The formation of the sp^3-like bond connecting the nearest-neighbor Al atoms was confirmed from the charge density distribution as in the cases of previous reports. The Young's modulus for single crystal AlLi was the highest in the $\langle 111 \rangle$ direction. The ratio of the Young's modulus for the $\langle 111 \rangle$ direction to that for the $\langle 100 \rangle$ direction, namely the elastic anisotropy E_{111}/E_{100}, was compared with those of the sp^3 bonded semiconductors such as Si and GaAs. The elastic anisotropy E_{111}/E_{100} of AlLi was lager than those of the sp^3 bonded semiconductors.

REFERENCES

1) K. Kishio and J. O. Brittain: Mater. Sci. Eng. **49** (1981) 1–6.
2) K. Kishio and J. O. Brittain: J. Phys. Chem. Solids **40** (1979) 933–940.
3) K. Kuriyama, S. Saito and K. Iwamura: J. Phys. Chem. Solids **40** (1979) 457–461.
4) E. D. Levine and E. J. Rapperport: Trans. Metall. AIME **227** (1963) 1204–1208.
5) E. Zintl and B. Brauer: Z. Phys. Chem. B (Leipzig) **20** (1933) 245–271.
6) W. Huckel: *Structural chemistry of inorganic compounds*, (Elsevier, Amsterdam, 1951) p. 829.
7) T. Asada, T. Jarlborg and A. J. Freeman: Phys. Rev. B **24** (1981) 510–516.
8) J. Hafner and W. Weber: Phys. Rev. B **33** (1986) 747–754.
9) A. Zunger: Phys. Rev. B **17** (1978) 2582–2594.
10) X. Q. Guo, R. Podloucky and A. J. Freeman: Phys. Rev. B **40** (1989) 2793–2800.
11) E. A. Starke and T. H. Sanders (Eds.): *Aluminum-Lithium Alloys, Proceedings of the First International Aluminum-Lithium Conference*, (Metallurgical Society of AIME, New York, 1981).
12) E. A. Starke and T. H. Sanders (Eds.): *Aluminum-Lithium Alloys II, Proceedings of the Second International Aluminum-Lithium Conference*, (Metallurgical Society of AIME, New York, 1984).
13) C. Baker, P. J. Gregson, C. J. Peel and S. J. Harris (Eds.): *Aluminum-Lithium Alloys III, Proceedings of the Third International Aluminum-Lithium Conference*, (Institute of Metals, London, 1985).
14) A. Arya, G. P. Das, H. G. Salunke and S. Banerjee: J. Phys.: Condens. Matter **6** (1994) 3389–3402.
15) G. P. Das, A. Arya and S. Banerjee: Intermetallics **4** (1996) 625–634.
16) N. E. Christensen: Phys. Rev. B **32** (1985) 207–228.
17) M. Sluiter, D. Defontaine, X. Q. Guo, R. Podloucky and A. J. Freeman: Phys. Rev. B **42** (1990) 10460–10476.
18) M. H. F. Sluiter, Y. Watanabe, D. Fontaine and Y. Kawazoe: Phys. Rev. B **53** (1996) 6137–6151.
19) A. K. Vasudevan and R. D. Doherty: Acta Metall. **35** (1987) 1193–1219.
20) A. K. Vasudevan, E. A. Ludwiczak, S. F. Baumann, R. D. Doherty and M. M. Kersker: Mater. Sci. Eng. **72** (1985) L25–L30.
21) A. Takahashi, T. Kobayashi and H. Toda: JJILM **49** (1999) 166–171.
22) K. Tanaka, T. Mori and T. Nakamura: Philos. Mag. **21** (1970) 267–279.
23) J. Y. Duan and Z. H. Li: Int. J. Fract. **115** (2002) L75–L80.
24) K. Masuda-Jindo and K. Terakura: Phys. Rev. B **39** (1989) 7509–7516.
25) T. Uesugi, M. Kohyama, M. Kohzu and K. Higashi: Mater. Trans. **42** (2001) 1167–1171.
26) M. J. Mehl: Phys. Rev. B **47** (1993) 2493–2500.
27) C. L. Fu, J. Zou and M. H. Yoo: Scr. Metall. Mater. **33** (1995) 885–891.
28) S. Tanaka, R. Yang, M. Kohyama, T. Sasaki, K. Matsunaga and Y. Ikuhara: Mater. Trans. **45** (2004) 1973–1977.
29) T. Yamamoto, F. Yamashita, I. Tanaka, E. Matsubara and A. Muramatsu: Mater. Trans. **45** (2004) 1987–1990.
30) T. Mohri and Y. Chen: Mater. Trans. **45** (2004) 1478–1484.
31) M. Mizuno, H. Araki and Y. Shirai: Mater. Trans. **45** (2004) 1964–1967.
32) H. Yoshida, H. Nagayama, A. Kuwabara and T. Sakuma: Mater. Trans. **45** (2004) 2106–2111.
33) S. Ishii, K. Ohno and Y. Kawazoe: Mater. Trans. **45** (2004) 1411–1413.
34) T. Hoshino, T. Mizuno, M. Asato and H. Fukushima: Mater. Trans. **42** (2001) 2206–2215.
35) O. Beckstein, J. E. Klepeis, G. L. W. Hart and O. Pankratov: Phys. Rev. B **63** (2001) 134112.
36) Y. Lee and B. N. Harmon: J. Alloy. Compd. **338** (2002) 242–247.
37) B. Holm, R. Ahuja, Y. Yourdshahyan, B. Johansson and B. I. Lundqvist: Phys. Rev. B **59** (1999) 12777–12787.
38) P. Baranek, J. Schamps and I. Noiret: J. Phys. Chem. B **101** (1997) 9147–9152.
39) S. Hong and C. L. Fu: Intermetallics **7** (1999) 5–9.
40) D. Y. Cheng, S. Q. Wang and H. Q. Ye: J. Alloy. Compd. **377** (2004) 221–224.
41) C. L. Fu: J. Mater. Res. **5** (1990) 971–979.
42) M. C. Payne, M. P. Teter, D. C. Allan, T. A. Arias and J. D. Joannopoulos: Rev. Mod. Phys. **64** (1992) 1045–1097.
43) P. Hohenberg and W. Kohn: Phys. Rev. **136** (1964) B864–B871.
44) W. Kohn and L. J. Sham: Phys. Rev. **140** (1965) A1133–A1138.
45) J. P. Perdew, J. A. Chevary, S. H. Vosko, K. A. Jackson, M. R. Pederson, D. J. Singh and C. Fiolhais: Phys. Rev. B **46** (1992) 6671–6687.
46) N. Troullier and J. L. Martins: Phys. Rev. B **43** (1991) 1993–2006.
47) D. Vanderbilt: Phys. Rev. B **41** (1990) 7892–7895.
48) H. J. Monkhorst and J. D. Pack: Phys. Rev. B **13** (1976) 5188–5192.
49) O. H. Nielsen and R. M. Martin: Phys. Rev. B **32** (1985) 3780–3791.
50) O. H. Nielsen and R. M. Martin: Phys. Rev. B **32** (1985) 3792–3805.
51) T. H. Fischer and J. Almlof: J. Phys. Chem. **96** (1992) 9768–9774.
52) R. Hill: Proc. Phys. Soc. London Sect. A **65** (1952) 349–354.
53) O. L. Anderson: J. Phys. Chem. Solids **24** (1979) 909–917.
54) R. Hearmon: Adv. Phys. **5** (1956) 323–381.
55) J. M. J. den Toonder, J. A. W. van Dommelen and F. P. T. Baaijens: Model. Simul. Mater. Sci. Eng. **7** (1999) 909–928.
56) S. V. Divinski and V. N. Dnieprenko: J. Phys.: Condens. Matter **6** (1994) 8503–8512.
57) R. L. Mullen, R. Ballarini, Y. Yin and A. H. Heuer: Acta Mater. **45** (1997) 2247–2255.
58) W. R. L. Lambrecht, B. Segall, M. Methfessel and M. V. Schilfgaarde: Phys. Rev. B **44** (1991) 3685–3694.
59) M. Nakamura and K. Kimura: J. Mater. Sci. **26** (1991) 2208–2214.
60) K. Kuriyama and S. Saito: Phys. Rev. B **13** (1976) 1528–1531.
61) S. P. Nikanorov, Y. A. Burenkov and A. V. Stepanov: Sov. Phys. Solid State **13** (1972) 2516–2518.
62) Y. A. Burenkov, Y. M. Burdukov, S. Y. Davidov and S. P. Nikanorov: Sov. Phys. Solid State **15** (1973) 1175–1177.
63) L. J. Slutsky and C. W. Garland: Phys. Rev. **113** (1959) 167–169.
64) W. L. Bond, W. P. Mason, H. J. McSkimin, K. M. Olsen and G. K. Teal: Phys. Rev. **78** (1950) 176.